

Observation of an enhancement in $e^+e^- \rightarrow \Upsilon(1S)\pi^+\pi^-$, $\Upsilon(2S)\pi^+\pi^-$, and $\Upsilon(3S)\pi^+\pi^-$ production around $\sqrt{s} = 10.89$ GeV at Belle

K.-F. Chen,²⁷ W.-S. Hou,²⁷ I. Adachi,⁸ H. Aihara,⁴⁴ T. Aushev,^{18,13} A. M. Bakich,⁴⁰ V. Balagura,¹³ A. Bay,¹⁸ K. Belous,¹² V. Bhardwaj,³⁴ M. Bischofberger,²⁴ A. Bondar,^{1,32} A. Bozek,²⁸ M. Bračko,^{20,14} J. Brodzicka,²⁸ T. E. Browder,⁷ M.-C. Chang,³ P. Chang,²⁷ Y. Chao,²⁷ A. Chen,²⁵ P. Chen,²⁷ B. G. Cheon,⁶ C.-C. Chiang,²⁷ R. Chistov,¹³ I.-S. Cho,⁴⁸ Y. Choi,³⁹ J. Dalseno,^{21,41} A. Drutskoy,² S. Eidelman,^{1,32} D. Epifanov,^{1,32} N. Gabyshev,^{1,32} P. Goldenzweig,² H. Ha,¹⁶ B.-Y. Han,¹⁶ K. Hayasaka,²³ H. Hayashii,²⁴ M. Hazumi,⁸ Y. Hoshi,⁴³ Y. B. Hsiung,²⁷ H. J. Hyun,¹⁷ T. Iijima,²³ K. Inami,²³ R. Itoh,⁸ M. Iwabuchi,⁴⁸ Y. Iwasaki,⁸ T. Julius,²² D. H. Kah,¹⁷ J. H. Kang,⁴⁸ N. Katayama,⁸ C. Kiesling,²¹ H. O. Kim,¹⁷ Y. I. Kim,¹⁷ Y. J. Kim,⁵ K. Kinoshita,² B. R. Ko,¹⁶ S. Korpar,^{20,14} P. Križan,^{19,14} P. Krokovny,⁸ Y.-J. Kwon,⁴⁸ S.-H. Kyeong,⁴⁸ J. S. Lange,⁴ S.-H. Lee,¹⁶ J. Li,⁷ C. Liu,³⁷ Y. Liu,²³ D. Liventsev,¹³ R. Louvot,¹⁸ J. MacNaughton,⁸ A. Matyja,²⁸ S. McOnie,⁴⁰ K. Miyabayashi,²⁴ H. Miyata,³⁰ Y. Miyazaki,²³ R. Mizuk,¹³ Y. Nagasaka,⁹ E. Nakano,³³ M. Nakao,⁸ S. Nishida,⁸ K. Nishimura,⁷ O. Nitoh,⁴⁶ T. Nozaki,⁸ S. Ogawa,⁴² T. Ohshima,²³ S. Okuno,¹⁵ G. Pakhlova,¹³ H. Park,¹⁷ H. K. Park,¹⁷ R. Pestotnik,¹⁴ M. Petrič,¹⁴ L. E. Piilonen,⁴⁷ S. Ryu,³⁸ H. Sahoo,⁷ K. Sakai,³⁰ Y. Sakai,⁸ O. Schneider,¹⁸ C. Schwanda,¹¹ A. J. Schwartz,² R. Seidl,³⁵ K. Senyo,²³ M. Shapkin,¹² C. P. Shen,⁷ J.-G. Shiu,²⁷ B. Shwartz,^{1,32} P. Smerkol,¹⁴ A. Sokolov,¹² E. Solovieva,¹³ S. Stanič,³¹ M. Starič,¹⁴ K. Sumisawa,⁸ T. Sumiyoshi,⁴⁵ S. Suzuki,³⁶ Y. Teramoto,³³ K. Trabelsi,⁸ S. Uehara,⁸ T. Uglov,¹³ Y. Unno,⁶ S. Uno,⁸ Y. Ushiroda,⁸ G. Varner,⁷ K. E. Varvell,⁴⁰ K. Vervink,¹⁸ C. H. Wang,²⁶ M.-Z. Wang,²⁷ P. Wang,¹⁰ Y. Watanabe,¹⁵ R. Wedd,²² J. Wicht,⁸ E. Won,¹⁶ B. D. Yabsley,⁴⁰ Y. Yamashita,²⁹ C. Z. Yuan,¹⁰ Z. P. Zhang,³⁷ V. Zhulanov,^{1,32} A. Zupanc,¹⁴ and O. Zyukova^{1,32}

(The Belle Collaboration)

¹*Budker Institute of Nuclear Physics, Novosibirsk*

²*University of Cincinnati, Cincinnati, Ohio 45221*

³*Department of Physics, Fu Jen Catholic University, Taipei*

⁴*Justus-Liebig-Universität Gießen, Gießen*

⁵*The Graduate University for Advanced Studies, Hayama*

⁶*Hanyang University, Seoul*

⁷*University of Hawaii, Honolulu, Hawaii 96822*

⁸*High Energy Accelerator Research Organization (KEK), Tsukuba*

⁹*Hiroshima Institute of Technology, Hiroshima*

¹⁰*Institute of High Energy Physics, Chinese Academy of Sciences, Beijing*

¹¹*Institute of High Energy Physics, Vienna*

¹²*Institute of High Energy Physics, Protvino*

¹³*Institute for Theoretical and Experimental Physics, Moscow*

¹⁴*J. Stefan Institute, Ljubljana*

¹⁵*Kanagawa University, Yokohama*

¹⁶*Korea University, Seoul*

¹⁷*Kyungpook National University, Taegu*

¹⁸*École Polytechnique Fédérale de Lausanne (EPFL), Lausanne*

¹⁹*Faculty of Mathematics and Physics, University of Ljubljana, Ljubljana*

²⁰*University of Maribor, Maribor*

²¹*Max-Planck-Institut für Physik, München*

²²*University of Melbourne, School of Physics, Victoria 3010*

²³*Nagoya University, Nagoya*

²⁴*Nara Women's University, Nara*

²⁵*National Central University, Chung-li*

²⁶*National United University, Miao Li*

²⁷*Department of Physics, National Taiwan University, Taipei*

²⁸*H. Niewodniczanski Institute of Nuclear Physics, Krakow*

²⁹*Nippon Dental University, Niigata*

³⁰*Niigata University, Niigata*

³¹*University of Nova Gorica, Nova Gorica*

³²*Novosibirsk State University, Novosibirsk*

³³*Osaka City University, Osaka*

³⁴*Panjab University, Chandigarh*

³⁵*RIKEN BNL Research Center, Upton, New York 11973*

³⁶*Saga University, Saga*

³⁷*University of Science and Technology of China, Hefei*

³⁸*Seoul National University, Seoul*

³⁹*Sungkyunkwan University, Suwon*

⁴⁰*School of Physics, University of Sydney, NSW 2006*

⁴¹*Excellence Cluster Universe, Technische Universität München, Garching*

⁴²*Toho University, Funabashi*

⁴³*Tohoku Gakuin University, Tagajo*

⁴⁴*Department of Physics, University of Tokyo, Tokyo*

⁴⁵*Tokyo Metropolitan University, Tokyo*

⁴⁶*Tokyo University of Agriculture and Technology, Tokyo*

⁴⁷*IPNAS, Virginia Polytechnic Institute and State University, Blacksburg, Virginia 24061*

⁴⁸*Yonsei University, Seoul*

We measure the production cross sections for $e^+e^- \rightarrow \Upsilon(1S)\pi^+\pi^-$, $\Upsilon(2S)\pi^+\pi^-$, and $\Upsilon(3S)\pi^+\pi^-$ as a function of \sqrt{s} between 10.83 GeV and 11.02 GeV. The data consists of 8.1 fb^{-1} collected with the Belle detector at the KEKB e^+e^- collider. We observe enhanced production in all three final states that does not conform well with the conventional $\Upsilon(10860)$ lineshape. A fit using a Breit-Wigner resonance shape yields a peak mass of $[10888.4_{-2.6}^{+2.7}(\text{stat}) \pm 1.2(\text{syst})] \text{ MeV}/c^2$ and a width of $[30.7_{-7.0}^{+8.3}(\text{stat}) \pm 3.1(\text{syst})] \text{ MeV}/c^2$.

PACS numbers: 13.25.Gv, 14.40.Pq

A host of new charmonium-like mesons have been discovered recently that do not seem to fit into the conventional $c\bar{c}$ spectrum. Possible interpretations for these exotic states include multi-quark states, mesonic-molecules ($c\bar{q}-\bar{c}q$, where q represents a u -, d - or s -quark), or $c\bar{c}g$ “hybrids” (where g is a gluon). The narrow $X(3872)$ [1], and various vector mesons, in particular, the broad $Y(4260)$ [2–4] resonance, were revealed by their dipion transitions to J/ψ (and ψ'). By analogy with the $Y(4260)$ discovery, it was suggested that a hidden-beauty counterpart, denoted Y_b [5], could be searched for in radiative return events from e^+e^- at center-of-mass (CM) energy on the $\Upsilon(10860)$ peak, or by an energy scan above it.

Analyzing a data sample recorded by the Belle detector at a single CM energy \sqrt{s} near the $\Upsilon(10860)$ resonance peak, no unusual structure was observed below the peak. Instead, anomalously large $\Upsilon(1S)\pi^+\pi^-$ and $\Upsilon(2S)\pi^+\pi^-$ production rates were observed [6]. If these signals are attributed entirely to dipion transitions from the $\Upsilon(10860)$ resonance, the corresponding partial widths would be two orders of magnitude larger than those for corresponding transitions from the $\Upsilon(2S)$, $\Upsilon(3S)$, and $\Upsilon(4S)$ states. Possible explanations include a new non-perturbative approach [7] to the decay widths of dipion transitions of heavy quarkonia, the presence of final state interactions [8], or the existence of a tetraquark state [9, 10]. A measurement of the energy dependence of the cross sections for $e^+e^- \rightarrow \Upsilon(nS)\pi^+\pi^-$ ($n = 1, 2, 3$) in and above the $\Upsilon(10860)$ energy region will provide more information for exploring these models.

Here we report the observation of the production of $e^+e^- \rightarrow \Upsilon(1S)\pi^+\pi^-$, $\Upsilon(2S)\pi^+\pi^-$, and $\Upsilon(3S)\pi^+\pi^-$ at $\sqrt{s} \simeq 10.83, 10.87, 10.88, 10.90, 10.93, 10.96,$ and 11.02 GeV, while the previous data collected at $\sqrt{s} \simeq 10.87$

GeV was already reported in Ref. [6].

The new 8.1 fb^{-1} data sample was also collected with the Belle detector at the KEKB e^+e^- collider [11]. In addition, nine scan points with an integrated luminosity of $\simeq 30 \text{ pb}^{-1}$ each, collected in the range of $\sqrt{s} = 10.80$ – 11.02 GeV, are used to obtain the hadronic line shape of the $\Upsilon(10860)$.

The Belle detector is a large-solid-angle magnetic spectrometer that consists of a silicon vertex detector (SVD), a central drift chamber (CDC), an array of aerogel threshold Cherenkov counters (ACC), a barrel-like arrangement of time-of-flight scintillation counters (TOF), and an electromagnetic calorimeter (ECL) comprised of CsI(Tl) crystals located inside a superconducting solenoid that provides a 1.5 T magnetic field. An iron flux-return located outside the coil is instrumented to detect K_L^0 mesons and to identify muons (KLM). The detector is described in detail elsewhere [12].

Events with four well-reconstructed charged tracks and zero net charge are selected to study $\Upsilon(nS)\pi^+\pi^-$ production. A final state that is consistent with a $\Upsilon(nS)$ candidate and two charged pions is reconstructed. A $\Upsilon(nS)$ candidate is formed from two muons with opposite charge, where the muon candidates are required to have associated hits in the KLM detector that agree with the extrapolated trajectory of a charged track provided by the drift chamber. The other two charged tracks must have a low likelihood of being electrons (the likelihood is calculated based on the ratio of ECL shower energy to the track momentum, dE/dx from the CDC, and the ACC response); they are then treated as pion candidates. This suppresses the background from $e^+e^- \rightarrow \mu^+\mu^-\gamma \rightarrow \mu^+\mu^-e^+e^-$ with a photon conversion. The cosine of the opening angle between the π^+ and π^- momenta in the laboratory frame is required to

TABLE I: CM energy (\sqrt{s}), integrated luminosity (\mathcal{L}), signal yield (N_s), reconstruction efficiency, and measured cross section (σ) for $e^+e^- \rightarrow \Upsilon(1S)\pi^+\pi^-$, $\Upsilon(2S)\pi^+\pi^-$, and $\Upsilon(3S)\pi^+\pi^-$. Due to a negative yield, an upper limit at 90% confidence level for $\sigma[e^+e^- \rightarrow \Upsilon(3S)\pi^+\pi^-]$ at $\sqrt{s} = 10.9555$ GeV is given.

\sqrt{s} (GeV)	\mathcal{L} (fb $^{-1}$)	$e^+e^- \rightarrow \Upsilon(1S)\pi^+\pi^-$			$e^+e^- \rightarrow \Upsilon(2S)\pi^+\pi^-$			$e^+e^- \rightarrow \Upsilon(3S)\pi^+\pi^-$		
		N_s	Eff.(%)	σ (pb)	N_s	Eff.(%)	σ (pb)	N_s	Eff.(%)	σ (pb)
10.8255	1.73	$10.6^{+4.0}_{-3.2}$	43.8	$0.56^{+0.21}_{-0.18} \pm 0.06$	$24.0^{+5.6}_{-4.9}$	34.9	$2.05^{+0.48}_{-0.42} \pm 0.24$	$1.8^{+1.8}_{-1.1}$	20.5	$0.23^{+0.23}_{-0.14} \pm 0.03$
10.8805	1.89	$43.4^{+7.2}_{-6.5}$	43.1	$2.14^{+0.36}_{-0.32} \pm 0.15$	$68.8^{+9.0}_{-8.3}$	35.4	$5.31^{+0.69}_{-0.64} \pm 0.59$	$14.9^{+4.3}_{-3.7}$	24.5	$1.47^{+0.43}_{-0.37} \pm 0.18$
10.8955	1.46	$26.2^{+5.8}_{-5.1}$	43.2	$1.68^{+0.37}_{-0.33} \pm 0.13$	$45.4^{+7.4}_{-6.7}$	35.6	$4.53^{+0.74}_{-0.67} \pm 0.51$	$10.3^{+3.7}_{-3.1}$	25.7	$1.26^{+0.45}_{-0.38} \pm 0.15$
10.9255	1.18	$11.1^{+4.0}_{-3.3}$	42.6	$0.89^{+0.32}_{-0.27} \pm 0.08$	$9.7^{+3.8}_{-3.1}$	35.9	$1.19^{+0.47}_{-0.38} \pm 0.16$	$2.9^{+2.2}_{-1.5}$	27.5	$0.41^{+0.31}_{-0.21} \pm 0.05$
10.9555	0.99	$3.9^{+2.6}_{-1.9}$	42.5	$0.37^{+0.25}_{-0.18} \pm 0.04$	$2.0^{+2.0}_{-1.3}$	36.4	$0.29^{+0.29}_{-0.19} \pm 0.05$	$-1.8^{+2.5}_{-3.0}$	29.4	$-0.28^{+0.39}_{-0.47} \pm 0.03 < 0.20$
11.0155	0.88	$4.9^{+2.8}_{-2.1}$	42.0	$0.53^{+0.31}_{-0.23} \pm 0.05$	$5.5^{+3.1}_{-2.4}$	36.0	$0.90^{+0.51}_{-0.39} \pm 0.17$	$4.3^{+2.6}_{-1.9}$	32.7	$0.69^{+0.42}_{-0.30} \pm 0.08$
10.8670	21.74	325^{+20}_{-19}	37.4	$1.61 \pm 0.10 \pm 0.12$	186 ± 15	18.9	$2.35 \pm 0.19 \pm 0.32$	$10.5^{+4.0}_{-3.3}$	1.5	$1.44^{+0.55}_{-0.45} \pm 0.19$

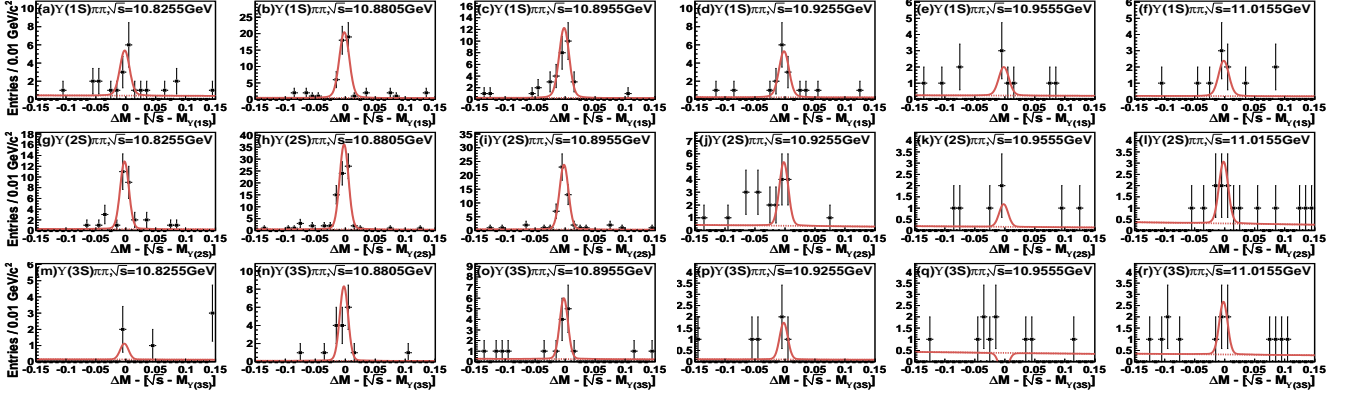


FIG. 1: The distributions of $\Delta M - [\sqrt{s} - M_{\Upsilon(nS)}]$ ($n = 1, 2, 3$) for (a–f) $\Upsilon(1S)\pi^+\pi^-$, (g–l) $\Upsilon(2S)\pi^+\pi^-$, and (m–r) $\Upsilon(3S)\pi^+\pi^-$ events with the fit results superimposed. The six columns of plots represent the data samples collected at different CM energies. The dashed curves show the background components in the fits.

be less than 0.95. The four-track invariant mass must satisfy $|M(\mu^+\mu^-\pi^+\pi^-) - \sqrt{s}| < 150$ MeV/ c^2 . The trigger efficiency for four-track events satisfying these criteria is very close to 100%.

The kinematic variable ΔM , defined by the difference between $M(\mu^+\mu^-\pi^+\pi^-)$ and $M(\mu^+\mu^-)$, is used to identify the signal candidates. Sharp signal peaks are expected at $\Delta M = \sqrt{s} - M_{\Upsilon(nS)}$. The candidate events are separated into three distinct regions defined by $|\Delta M - [\sqrt{s} - M_{\Upsilon(nS)}]| < 150$ MeV/ c^2 for $n = 1, 2$, and 3, and signal yields are extracted from an unbinned extended maximum likelihood (ML) fit to the ΔM distribution within each region. The likelihood function for each fit is defined as

$$L(N_s, N_b) = \frac{e^{-(N_s+N_b)}}{N!} \prod_{i=1}^N [N_s \cdot P_s(\Delta M_i) + N_b \cdot P_b(\Delta M_i)],$$

where N_s (N_b) denotes the yield for signal (background), and P_s (P_b) is the signal (background) probability density function (PDF). The signal is modelled by a sum of two Gaussians while the background is approximated by

a linear function. The Gaussians parameterized for the signal PDF are fixed from the Monte Carlo (MC) simulation at each energy point. We fit 18 ΔM distributions (shown in Fig. 1 with the fit results superimposed) simultaneously with common corrections to the mean and width of the signal Gaussians.

The measured signal yields, reconstruction efficiencies, integrated luminosity, and the production cross sections, as well as the results from the previous publication [6] for the data sample collected at $\sqrt{s} = 10.867$ GeV, are summarized in Table I. The efficiencies for $\Upsilon(3S)\pi^+\pi^-$ are much improved compared to Ref. [6] as the inefficient selection criterion $\theta_{\max} < 175^\circ$ has been removed, where θ_{\max} is the maximum opening angle between any pair of charged tracks in the CM frame.

For the cross section measurements, systematic uncertainties are dominated by the $\Upsilon(nS) \rightarrow \mu^+\mu^-$ branching fractions, reconstruction efficiencies, and PDF parameterization for the fits. Uncertainties of 2.0%, 8.8%, and 9.6% for the $\Upsilon(1S)$, $\Upsilon(2S)$, and $\Upsilon(3S) \rightarrow \mu^+\mu^-$ branching fractions are included, respectively. For the $\Upsilon(1S)\pi^+\pi^-$ and $\Upsilon(2S)\pi^+\pi^-$ modes, the reconstruction

efficiencies are obtained from MC simulations using the observed $M(\pi^+\pi^-)$ and $\cos\theta_{\text{Hel}}$ (the angle between the π^- and $\Upsilon(10860)$ momenta in the $\pi^+\pi^-$ rest frame) distributions in our previous publication as inputs [6]. The uncertainties associated with these distributions give rise to 2.7%–4.5% and 1.9%–4.2% uncertainties for the $\Upsilon(1S)\pi^+\pi^-$ and $\Upsilon(2S)\pi^+\pi^-$ efficiencies, respectively. The ranges on the uncertainty arise from the CM energy dependence of the $\pi^+\pi^-$ system. We use the model of Ref. [13] as well as a phase space model as inputs for $\Upsilon(3S)\pi^+\pi^-$ measurements; the differences in acceptance are included as systematic uncertainties. The uncertainties from the PDF parameterization are estimated either by replacing the signal PDF with a sum of three Gaussians, or by replacing the background PDF with a second-order polynomial. The differences between these alternative fits and the nominal results are taken as the systematic uncertainties. Other uncertainties include: tracking efficiency (1% per charged track), muon identification (0.5% per muon candidate), electron rejection for the charged pions (0.1–0.2% per pion), trigger efficiencies (0.1–5.2%), and integrated luminosity (1.4%). The uncertainties from all sources are added in quadrature. The total systematic uncertainties are 7%–11%, 11%–16%, and 12%–14% for the $\Upsilon(1S)\pi^+\pi^-$, $\Upsilon(2S)\pi^+\pi^-$, and $\Upsilon(3S)\pi^+\pi^-$ channels, respectively.

In order to extract the resonance shape, we perform a χ^2 fit to the measured production cross sections, including the one estimated at $\sqrt{s} = 10.867$ GeV, using the model $\sigma_{\Upsilon(nS)\pi\pi}/\sigma_{\mu\mu}^0 \propto A_{\Upsilon(nS)\pi\pi} |R_0 + e^{i\phi} BW(\mu, \Gamma)|^2$, where $\sigma_{\mu\mu}^0 = 4\pi\alpha^2/3s$ is the leading-order $e^+e^- \rightarrow \mu^+\mu^-$ cross section and $BW(\mu, \Gamma)$ is the Breit-Wigner function $1/[(s - \mu^2) + i\mu\Gamma]$. The normalizations for $\Upsilon(1S)\pi^+\pi^-$, $\Upsilon(2S)\pi^+\pi^-$, and $\Upsilon(3S)\pi^+\pi^-$ ($A_{\Upsilon(nS)\pi\pi}$), as well as the amplitude of the flat component R_0 , the mean μ , width Γ , and the complex phase ϕ of the parent resonance are free parameters in the fit. Because of the low statistics, common resonance parameters are introduced for the three different final states. Results of the fits, shown as the smooth curves in Fig. 2, are summarized in Table II. The fit quality is $\chi^2 = 24.6$ for 14 degrees of freedom. An alternative fit without the last data point collected at $\sqrt{s} \sim 11.02$ GeV yields a similar result, $\mu = 10889.0^{+5.8}_{-2.9}$ MeV/ c^2 , $\Gamma = 37^{+16}_{-10}$ MeV/ c^2 , and $\chi^2 = 21.3$ for 11 degrees of freedom. Systematic uncertainties associated with the cross section measurements are propagated to the resonance shapes. The fits are repeated, and the variations on the shape parameters are included as the systematic uncertainties. In addition to the uncertainties on the cross sections, the beam energy around $\Upsilon(10860)$ is measured by $M_{\Upsilon(nS)} + \Delta M$ in the $\Upsilon(nS)\pi^+\pi^-$ events, and an uncertainty of ± 1 MeV is included. For the scan data, a common energy shift is also obtained from the fit to $\Upsilon(nS)\pi^+\pi^-$ events. The relative beam energies are further checked using the $M(\mu^+\mu^-)$ distributions of

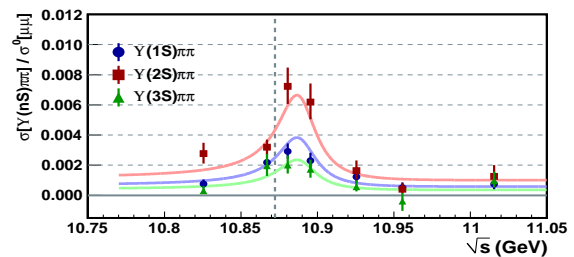


FIG. 2: The CM energy-dependent cross sections for $e^+e^- \rightarrow \Upsilon(nS)\pi^+\pi^-$ ($n = 1, 2, 3$) processes normalized to the leading-order $e^+e^- \rightarrow \mu^+\mu^-$ cross sections. The results of the fits are shown as smooth curves. The vertical dashed line indicates the energy at which the hadronic cross section is maximal.

μ -pair samples.

The resonance parameters for the $\Upsilon(10860)$ are determined using energy scan data collected at CM energies between 10.80 and 11.02 GeV. We measure the fraction $R_b = \sigma_b/\sigma_{\mu\mu}^0$, where $\sigma_b = N_b^{R_2 < 0.2}(s)/\mathcal{L}\epsilon_b(s)$ is the $e^+e^- \rightarrow b\bar{b}$ hadronic cross section. The number of $e^+e^- \rightarrow b\bar{b}$ events with $R_2 < 0.2$ ($N_b^{R_2 < 0.2}$) is estimated by subtraction of non- $b\bar{b}$ events scaled from a data set collected at $\sqrt{s} \simeq 10.52$ GeV, where R_2 denotes the ratio of the second to zeroth Fox-Wolfram moments [14]. Selection criteria for hadronic events are described in Ref. [15]. The acceptance for $e^+e^- \rightarrow b\bar{b}$ ($\epsilon_b(s)$) is found to vary slightly from 68.1% to 70.5% over the range of scan energies. The line shape used to model our data is given by $|A_{nr}|^2 + |A_0 + A_{10860}e^{i\phi_{10860}} BW(\mu_{10860}, \Gamma_{10860}) + A_{11020}e^{i\phi_{11020}} BW(\mu_{11020}, \Gamma_{11020})|^2$; this parameterization is the same as that used in Ref. [16]. We perform a χ^2 fit to our R_b measurements as shown in Fig. 3(a). The shapes for $\Upsilon(11020)$ (ϕ_{11020} , μ_{11020} , and Γ_{11020}) are fixed to the values in Ref. [16], since our data points are not able to constrain the $\Upsilon(11020)$ parameters. The resulting shape parameters for the $\Upsilon(10860)$ are $\phi_{10860} = 2.33^{+0.26}_{-0.24}$

TABLE II: Cross sections (σ) at peak, mean (μ), width (Γ), phase (ϕ), and the amplitude for the constant component (R_0) from the fit to the CM energy-dependent $e^+e^- \rightarrow \Upsilon(1S)\pi^+\pi^-$, $\Upsilon(2S)\pi^+\pi^-$, and $\Upsilon(3S)\pi^+\pi^-$ cross sections. There are two solutions for ϕ and R_0 with identical χ^2 . The first uncertainty is statistical, and the second is systematic.

$\Upsilon(1S)\pi\pi$ σ at peak	$(2.78^{+0.42}_{-0.34} \pm 0.23)$ pb
$\Upsilon(2S)\pi\pi$ σ at peak	$(4.82^{+0.77}_{-0.62} \pm 0.66)$ pb
$\Upsilon(3S)\pi\pi$ σ at peak	$(1.71^{+0.35}_{-0.31} \pm 0.24)$ pb
μ	$(10888.4^{+2.7}_{-2.6} \pm 1.2)$ MeV/ c^2
Γ	$(30.7^{+8.3}_{-7.0} \pm 3.1)$ MeV/ c^2
ϕ	$(1.97 \pm 0.26 \pm 0.06)$ or $(-1.74 \pm 0.11 \pm 0.02)$ rad
R_0	$(1.98^{+0.72}_{-0.60} \pm 0.20)$ or $(0.87^{+0.29}_{-0.22} \pm 0.09)$ (GeV) $^{-2}$

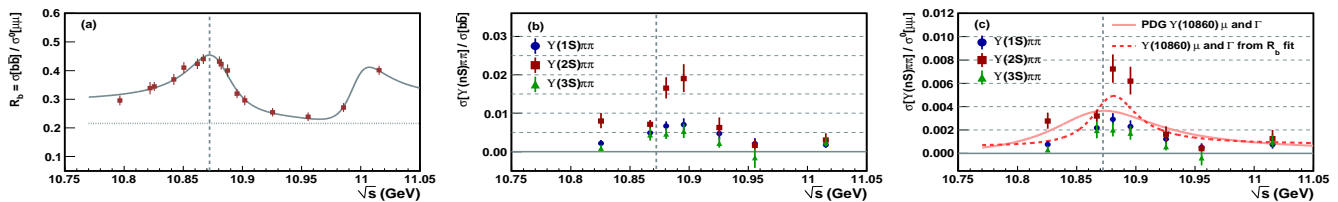


FIG. 3: (a) The R_b and (b) the ratio between $\sigma[e^+e^- \rightarrow \Upsilon(nS)\pi^+\pi^-]$ and $\sigma[e^+e^- \rightarrow b\bar{b}]$ as a function of CM energy; (c) the energy-dependent cross section ratios for $e^+e^- \rightarrow \Upsilon(nS)\pi^+\pi^-$ events, the result of fits with resonant parameters from R_b or PDG averages are superimposed. The horizontal dotted line in (a) is the non-interfering $|A_{nr}|^2$ contribution in the fit. The vertical dashed line indicates the energy at which the hadronic cross section is maximal.

rad, $\mu_{10860} = 10879 \pm 3 \text{ MeV}/c^2$, and $\Gamma_{10860} = 46_{-7}^{+9} \text{ MeV}/c^2$. These values are consistent with those obtained in Ref. [16]. The quality of the fit is $\chi^2 = 4.4$ for 9 degrees of freedom.

Figure 3(b) shows the ratio between $\sigma[e^+e^- \rightarrow \Upsilon(nS)\pi^+\pi^-]$ and $\sigma[e^+e^- \rightarrow b\bar{b}]$ as a function of CM energy. A fit to the $\Upsilon(nS)\pi\pi$ cross sections with $\mu_{\Upsilon(nS)\pi\pi} = \mu_{10860}$ and $\Gamma_{\Upsilon(nS)\pi\pi} = \Gamma_{10860}$ gives $\chi^2 = 37.8$ for 16 degrees of freedom as shown in Fig. 3(c). This corresponds to a deviation of 3.2σ from the nominal fit with floated $\mu_{\Upsilon(nS)\pi\pi}$ and $\Gamma_{\Upsilon(nS)\pi\pi}$. If we perform a scan within the region with $(\mu_{\Upsilon(nS)\pi\pi} - \mu_{10860})^2/\sigma(\mu_{10860})^2 + (\Gamma_{\Upsilon(nS)\pi\pi} - \Gamma_{10860})^2/\sigma(\Gamma_{10860})^2 \leq 1$, a minimum deviation of 2.3σ is found, where $\sigma(\mu_{10860})$ and $\sigma(\Gamma_{10860})$ are statistical. If the resonant mean and width are fixed to the results in Ref. [16] or PDG values [17], a deviation of 3.9σ or 5.6σ is obtained; scans within the 1σ bound yield a deviation of 3.4σ or 5.1σ .

In summary, we report the observation of enhanced $e^+e^- \rightarrow \Upsilon(1S)\pi^+\pi^-$, $\Upsilon(2S)\pi^+\pi^-$, and $\Upsilon(3S)\pi^+\pi^-$ production at CM energies between $\sqrt{s} \simeq 10.83$ and 11.02 GeV. The energy-dependent cross sections for $e^+e^- \rightarrow \Upsilon(nS)\pi^+\pi^-$ events are measured for the first time, and are found to differ from the shape of the $e^+e^- \rightarrow b\bar{b}$ cross section. A Breit-Wigner resonance shape fit yields a peak mass of $10888.4_{-2.6}^{+2.7}(\text{stat}) \pm 1.2(\text{syst}) \text{ MeV}/c^2$ and a width of $30.7_{-7.0}^{+8.3}(\text{stat}) \pm 3.1(\text{syst}) \text{ MeV}/c^2$. A fit excluding the $\sqrt{s} \sim 11.02$ GeV data point is consistent with the nominal fit, indicating no strong contribution of $\Upsilon(nS)\pi\pi$ events from $\Upsilon(11020)$. The $\Upsilon(10860)$ shape parameters obtained from our R_b hadronic cross section measurements are consistent with the measurements from BaBar. The differences between the shape parameters from $\Upsilon(nS)\pi\pi$ events and from our R_b measurements are $\mu_{\Upsilon(nS)\pi\pi} - \mu_{10860} = 9 \pm 4 \text{ MeV}/c^2$ and $\Gamma_{\Upsilon(nS)\pi\pi} - \Gamma_{10860} = -15_{-12}^{+11} \text{ MeV}/c^2$. A fit to the $e^+e^- \rightarrow \Upsilon(nS)\pi^+\pi^-$ cross sections with our measured $\Upsilon(10860)$ mean and width yields a deviation of 3.2σ , while a deviation of 2.3σ is obtained if we allow a maximal $\pm 1\sigma$ drift of the $\Upsilon(10860)$ shape parameters. The $\Upsilon(nS)\pi^+\pi^-$ partial widths were found to be much larger than the expectations for conventional $\Upsilon(5S)$ states. As

an extension, energy-dependent $\Upsilon(nS)\pi^+\pi^-$ production cross sections are measured; the observed structure deviates from the $\Upsilon(10860)$ shape obtained from the hadronic cross sections.

We thank the KEKB group for excellent operation of the accelerator, the KEK cryogenics group for efficient solenoid operations, and the KEK computer group and the NII for valuable computing and SINET3 network support. We acknowledge support from MEXT, JSPS and Nagoya's TLPRC (Japan); ARC and DIISR (Australia); NSFC (China); DST (India); MEST, KOSEF, KRF (Korea); MNiSW (Poland); MES and RFAAE (Russia); ARRS (Slovenia); SNSF (Switzerland); NSC and MOE (Taiwan); and DOE (USA).

-
- [1] S.-K. Choi *et al.* [Belle Collaboration], Phys. Rev. Lett. **91**, 262001 (2003).
 - [2] B. Aubert *et al.* [BaBar Collaboration], Phys. Rev. Lett. **95**, 142001 (2005).
 - [3] T. E. Coan *et al.* [CLEO Collaboration], Phys. Rev. Lett. **96** (2006) 162003.
 - [4] C. Z. Yuan *et al.* [Belle Collaboration], Phys. Rev. Lett. **99**, 182004 (2007).
 - [5] W.-S. Hou, Phys. Rev. D **74**, 017504 (2006).
 - [6] K.-F. Chen *et al.* [Belle Collaboration], Phys. Rev. Lett. **100**, 112001 (2008).
 - [7] Yu. A. Simonov, JETP Lett. **87**, 147 (2008).
 - [8] C. Meng and K.-T. Chao, Phys. Rev. D **77**, 074003 (2008); *ibid.* D **78**, 034022 (2008).
 - [9] M. Karliner and H. J. Lipkin, arXiv:0802.0649 [hep-ph].
 - [10] A. Ali, C. Hambrock, I. Ahmed and M. J. Aslam, Phys. Lett. B **684**, 28 (2010); A. Ali, C. Hambrock and M. J. Aslam, arXiv:0912.5016 [hep-ph].
 - [11] S. Kurokawa and E. Kikutani, Nucl. Instrum. Methods Phys. Res., Sect. A **499**, 1 (2003), and other papers included in this Volume.
 - [12] A. Abashian *et al.* [Belle Collaboration], Nucl. Instrum. Methods Phys. Res., Sect. A **479**, 117 (2002).
 - [13] L. S. Brown and R. N. Cahn, Phys. Rev. Lett. **35**, 1 (1975); M. B. Voloshin, JETP Lett. **21**, 347 (1975); Y.-P. Kuang and T.-M. Yan, Phys. Rev. D **24**, 2874 (1981).
 - [14] G. C. Fox and S. Wolfram, Phys. Rev. Lett. **41**, 1581 (1978).

- [15] K. Abe *et al.* [Belle Collaboration], Phys. Rev. Lett. **86**, 3228 (2001).
- [16] B. Aubert *et al.* [BaBar Collaboration], Phys. Rev. Lett. **102**, 012001 (2009).
- [17] C. Amsler *et al.* [Particle Data Group], Phys. Lett. B **667**, 1 (2008).